Marine Biotechnology
https://doi.org/10.1007/s10126-021-10059-y

ORIGINAL ARTICLE

Disentangling the Roles of Functional Domains in the Aggregation and Adsorption of the Multimodular Sea Star Adhesive Protein Sfp1

Mathilde Lefevre[1,2] · Thomas Ederth[3] · Thibault Masai[1] · Ruddy Wattiez[4] · Philippe Leclère[2] · Patrick Flammang[5] · Elise Hennebert[1]

Received: 19 June 2021 / Accepted: 16 August 2021

Abstract

Sea stars can adhere to various underwater substrata using an adhesive secretion of which Sfp1 is a major component. Sfp1 is a multimodular protein composed of four subunits (Sfp1 Alpha, Beta, Delta, and Gamma) displaying different functional domains. We recombinantly produced two fragments of Sfp1 comprising most of its functional domains: the C-terminal part of the Beta subunit (rSfp1 Beta C-term) and the Delta subunit (rSfp1 Delta). Surface plasmon resonance analyses of protein adsorption onto different model surfaces showed that rSfp1 Beta C-term exhibits a significantly higher adsorption than the fibrinogen control on hydrophobic, hydrophilic protein-resistant, and charged self-assembled monolayers, while rSfp1 Delta adsorbed more on negatively charged and on protein-resistant surfaces compared to fibrinogen. Truncated recombinant rSfp1 Beta C-term proteins were produced in order to investigate the role of the different functional domains in the adsorption of this protein. The analysis of their adsorption capacities on glass showed that two mechanisms are involved in rSfp1 Beta C-term adsorption: (1) one mediated by the EGF-like domain and involving Ca^{2+} and Mg^{2+} ions, and (2) one mediated by the sequence of Sfp1 Beta with no homology with known functional domain in databases, in the presence of Na^{+}, Ca^{2+} and Mg^{2+} ions.

Keywords Sea stars · Adhesive protein · Sfp1 · Functional domain · Adsorption · SPR

Introduction

Sea stars are benthic motile organisms occupying diverse marine habitats from the intertidal to the abyssal zones. To accomplish activities essential for their survival, i.e., locomotion, feeding, and attachment to withstand the action of waves, they rely on a proteinaceous adhesive substance released from their tube feet (Flammang et al. 1998). Sea star adhesion is defined as temporary because tube feet can also become detached voluntarily, allowing the sea star to move around. Contrary to sessile marine invertebrates relying on permanent adhesion and therefore staying at the same place throughout their lifetime (e.g., barnacles), sea stars may encounter various substrata during their displacements, and their adhesive secretions should be versatile to cope with surfaces of varying chemical and physical characteristics (Santos et al. 2009). In that way, sea stars naturally accomplish the objective of numerous human industries: the production of an efficient glue able to rapidly stick to surfaces with various properties under wet conditions (Wang et al. 2018; Claverie et al. 2020).

✉ Elise Hennebert
elise.hennebert@umons.ac.be

1 Laboratory of Cell Biology, Research Institute for Biosciences, University of Mons, Place du Parc 23, 7000 Mons, Belgium

2 Laboratory for Chemistry of Novel Materials, Center for Innovation and Research in Materials and Polymers (CIRMAP), Research Institute for Materials, University of Mons, 7000 Mons, Belgium

3 Division of Biophysics and Bioengineering, Department of Physics, Chemistry and Biology, Linköping University, 581 83 Linköping, Sweden

4 Laboratory of Proteomics and Microbiology, Research Institute for Biosciences, University of Mons, 7000 Mons, Belgium

5 Biology of Marine Organisms and Biomimetics Unit, Research Institute for Biosciences, University of Mons, 7000 Mons, Belgium

Published online: 15 September 2021

The composition of the adhesive secretion of the sea star *Asterias rubens* has been studied in detail. The use of high-throughput sequencing of expressed mRNAs (transcriptome analysis) combined with mass spectrometry analysis of the glue proteome identified 34 proteins composing this adhesive secretion, of which 22 were found to be exclusively expressed in the cells responsible for the secretion of the adhesive material (Hennebert et al. 2015; Lengerer et al. 2019). One of them, the sea star footprint protein-1 (Sfp1) has been characterized (Hennebert et al. 2014). It is the second-most abundant protein in the secreted adhesive where it makes up a structural scaffold deposited on a surface-coupling layer (Hennebert et al. 2008, 2014). Sfp1 is a large protein of 3853 amino acids cleaved into four subunits (Alpha, Beta, Gamma, Delta) which each display different functional domains (Hennebert et al. 2014). Altogether, 20 domains of seven different types are found in Sfp1: one farnesoic acid O-methyl transferase domain, two calcium-binding EGF-like domains, three galactose binding lectin domains, five discoidin domains (also known as F5/8 type C domains), three von Willebrand Factor type D (VWD) domains, three trypsin inhibitor-like (TIL) cysteine-rich domains, and three C8 domains (Hennebert et al. 2014). The major cohesive role of Sfp1 in sea star adhesion is also reflected by the fact that it is evolutionary conserved among distantly related sea stars, regardless of inhabited environments (Lengerer et al. 2019). Moreover, multimodular proteins depicting the same types of functional domains have been identified in adhesive secretions from sea urchins, flatworms, and sticklebacks, suggesting they are a common feature in some adhesive proteins (Seear et al. 2015; Wunderer et al. 2019; Pjeta et al. 2020).

Recently, we used the bacterium *Escherichia coli* to recombinantly produce two fragments of Sfp1 comprising most of its functional domains: the C-terminal part of the Beta subunit (rSfp1 Beta C-term) comprising two discoidin domains and one EGF domain, and the complete Delta subunit (rSfp1 Delta) comprising one VWD domain, one C8 domain, one TIL domain, and one galactose-binding lectin domain. Using native polyacrylamide gel electrophoresis and size exclusion chromatography, we showed that these proteins self-assemble to form oligomers and aggregates in the presence of NaCl. Moreover, they adsorbed onto glass and polystyrene surfaces upon addition of Na^+ and/or Ca^{2+} ions. We proposed that this behavior mimicks the self-assembly of the native sea star adhesive triggered by the change in salt concentration between the secretory granule environment where the proteins are stored in adhesive cells and the seawater external environment. This was clearly apparent for rSfp1 Beta C-term, for which adsorption increased with cation concentration and was the highest at the Na^+ and Ca^{2+} concentrations found in seawater (Lefevre et al. 2020). The coatings made up of each of the two recombinant proteins had no cytotoxic effects on HeLa cells and even increased their proliferation (Lefevre et al. 2020).

In this study, we characterized further the adsorption ability of these Sfp1 fragments. We used surface plasmon resonance (SPR) to analyze quantitatively the adsorption of rSfp1 Beta C-term and rSfp1 Delta in buffer conditions in which they form homogeneous films, i.e., Tris buffer supplemented with 450 mM NaCl or with 150 mM $CaCl_2$, respectively (Lefevre et al. 2020). We showed that, under these conditions, both proteins exhibit better adsorption to various surface chemistries than fibrinogen, a blood plasma protein used as a model protein in adsorption studies (Lowe et al. 2015; Horbett 2018). Based on these results, and to elucidate the function of each domain in rSfp1 Beta C-term, truncated rSfp1 Beta C-term proteins were produced, and their adsorption abilities on glass were assessed qualitatively. We showed that only the EGF domain and the unannotated sequence of rSfp1 Beta C-term are responsible for its adsorption abilities. Our results indicate that protein simplification is a promising way to disentangle the functional principles of large multidomain adhesive proteins, allowing to mimic them to develop new bio-inspired adhesives or coatings.

Materials and Methods

Production of Recombinant Proteins

Recombinant rSfp1 Beta C-term and rSfp1 Delta were expressed in *Escherichia coli* C2566 strain (New England Biolabs) and purified as previously described (Lefevre et al. 2020). Briefly, the corresponding coding sequences were cloned in pET-28a (+) protein expression vector (Novagen) in frame with C-terminal 6×His-tag coding sequence. The proteins were purified from bacterial inclusion bodies under denaturing conditions (8 M urea, 1 mM dithiothreitol (DTT) using a 1-mL HisTrap HP column (GE Healthcare) connected to an Äkta Start system (GE Healthcare). The purification steps were performed in the absence of NaCl for rSfp1 Beta C-term, and in the presence of NaCl for rSfp1 Delta, to prevent the precipitation of the proteins (Lefevre et al. 2020). After dialysis to remove urea and DTT, the proteins were stored at 4 °C in 25 mM Tris buffer, pH 8 before the experiments. In these conditions, rSfp1 Beta C-term form oligomers only while rSfp1 Delta is present in the form of a mix of oligomers, dimers, and monomers. For the latter recombinant protein, fractions corresponding to the monomer only or to a mix of monomers and dimers isolated by size exclusion chromatography were used (Lefevre et al. 2020).

To understand the role of each domain in the aggregation and adsorption mechanisms of rSfp1 Beta C-term, truncated recombinant proteins were produced. Four fragments were designed based on the functional domains of this protein: (1) the unannotated domain (hereby named "Unannotated"), (2) the second discoidin domain (hereby named "FA58C"), (3) the second discoidin domain followed by the EGF domain (hereby named "FA58C-EGF"), and (4) the unannotated domain flanked by the two discoidin domains (hereby named "FA58C-Unannotated-FA58C") (Figs. 1a and S1). The coding sequences for these 4 constructions were amplified by PCR using Q5 High-Fidelity DNA polymerase (New England Biolabs, Ipswich, MA, USA), generating an NdeI site with the forward primer and an XhoI site with the reverse primer (see Table S1 for the sequences of the primers used). The resulting PCR products (577 bp, 466 bp, 589 bp, and 1489 bp, respectively) were then cleaved by NdeI and XhoI restriction enzymes (Thermo Fisher Scientific) and ligated using T4 DNA ligase (Thermo Fisher Scientific) into the pET-28a (+) expression plasmid in frame with a C-terminal 6×His-tag coding sequence. The sequences of the inserts were confirmed by Sanger sequencing (Eurofins Genomics). The fragments were produced as described above and purified from inclusion bodies under denaturing conditions in the presence or absence of NaCl. The proteins were dialyzed extensively (i.e., with decreasing molarity of urea and DTT) or directly, both in the presence or absence of NaCl. The proteins were then stored at 4 °C in 25 mM Tris buffer, pH 8.

Protein concentrations were determined by UV spectroscopy after centrifugation using the following calculated extinction coefficients (protparam, www.expasy.org): 104,945 M^{-1} cm^{-1} for rSfp1 Beta C-term, 59,020 M^{-1} cm^{-1} for rSfp1 Delta, 39,670 M^{-1} cm^{-1} for Unannotated, 24,075 M^{-1} cm^{-1} for FA58C, 31,440 M^{-1} cm^{-1} for FA58C-EGF, and 91,955 M^{-1} cm^{-1} for FA58C-Unannotated-FA58C. The identity and purity of recombinant proteins was verified using SDS-PAGE and mass spectrometry as previously described (Lefevre et al. 2020).

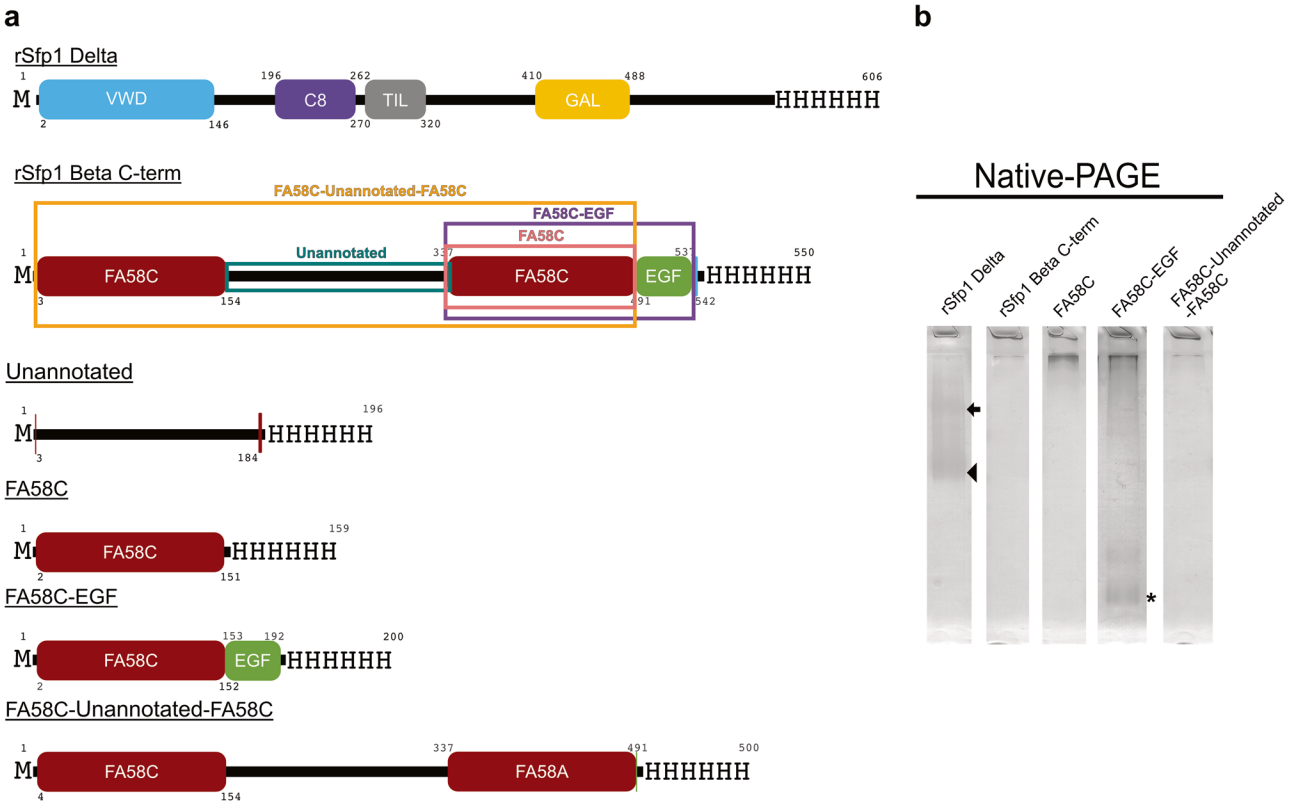

Fig. 1 Recombinant Sfp1 proteins investigated in this study. **a** Schematic views of rSfp1 Delta and of full-length and truncated rSfp1 Beta C-term. Unannotated, FA58C, FA58C-EGF, and FA58C-Unannotated-FA58C fragments of rSfp1 Beta C-term are framed in blue, pink, purple, and orange, respectively. Conserved domains predicted by the Conserved Domain Database are shown: blue: von Willebrand factor type D domain (VWD), purple: C8 domain, grey: trypsin inhibitor-like cysteine rich domain (TIL), orange: galactose binding lectin domain (GAL), burgundy: coagulation factor 5/8 C-terminal domain/discoidin domain (FA58C), green: calcium-binding EGF-like domain (EGF). **b** Native-PAGE analysis of recombinant proteins. Proteins were extracted from inclusion bodies, purified by immobilized-metal affinity chromatography, and dialyzed against 25 mM Tris. Ten micrograms of proteins was loaded on 12% Native-PAGE gels. The arrowhead indicates the monomer of rSfp1 Delta, the arrow indicates the dimer of Sfp1 Delta, and the asterisk indicates the monomer of FA58C-EGF. The Unannotated fragment precipitated during the purification and was not analyzed in Native-PAGE

Native-PAGE Analysis

After dialysis, all the recombinant proteins were analyzed by Native-PAGE electrophoresis to investigate the presence of monomers or oligomers. Proteins were suspended in 50 mM Tris–HCl (pH 6.8), 10% glycerol, 0.01% bromophenol blue, and centrifuged at 17,000 g for 5 min before loading. Electrophoresis was performed at 4 °C for 2 h, and the gels were stained with Coomassie brilliant blue R-250. The mixes of full-length or truncated rSfp1 Beta C-term with rSfp1 Delta, and of truncated rSfp1 Beta C-term proteins with NaCl, $CaCl_2$, and $MgCl_2$ were also investigated.

Surface Plasmon Resonance

Five types of self-assembled monolayers (SAMs) were chemically prepared for SPR experiments as described previously (Petrone et al. 2015; Tilbury et al. 2019, see Supplementary information). These surfaces exposed homogeneous methyl (CH_3), hydroxyl (OH), carboxyl (COOH), trimethylamine ($N(CH_3)_3$), or methoxylated PEG (EG11-Me, hence "mPEG") chemistries. SPR experiments were performed using a Biacore 3000 unit (GE Healthcare, Sweden) with a flow rate of 10 µL min^{-1} at 25 °C. Two different running buffers were used: 25 mM Tris, 450 mM NaCl pH 8.0 for rSfp1 Beta C-term and 25 mM Tris, 150 mM $CaCl_2$ pH 8.0 for rSfp1 Delta. These conditions were selected based on previous results of surface coating analyses on glass coverslips, where they induce the formation of homogeneous films of the two recombinant proteins (Lefevre et al. 2020). An equilibration phase with running buffer was performed for 5 min followed by the injection of 0.5 mg/mL protein samples for 5 min at 10 µl/min of flow rate at 25 °C. Finally, 1 min of dissociation phase with the same running buffer was applied. The adsorption of rSfp1 Beta C-term and rSfp1 Delta was compared to the adsorption of fibrinogen and BSA, used as controls. Adsorption in resonance units (ΔRU) was converted to adsorbed mass (m) via the following relation:

$$\Delta m = C_{SPR} \Delta RU$$

where C_{SPR} corresponds to 6.5×10^{-2} ng cm^{-2} for the adsorption of proteins to flat surfaces (Petrone et al. 2015).

The experiments were performed three times independently, and the mean ΔRU obtained for each SAM was analyzed by two-way analysis of variance (ANOVA) followed by the Tukey multiple comparison test. Analyses were performed with Prism 8.4.3 (GraphPad). Results were considered statistically significant at $P < 0.05$.

Qualitative Analysis of the Adsorption of Truncated rSfp1 Beta C-Term Proteins

Based on previous adsorption tests performed on rSfp1 Beta C-term (Lefevre et al. 2020), different conditions were selected to characterize the adsorption of truncated rSfp1 Beta C-term proteins by surface coating analysis. A 40-µL drop of a 0.2-mg/mL solution of each recombinant protein in Tris buffer was deposited onto glass coverslips pre-cleaned with 5% HCl and mixed with 40 µL of different buffers to generate the following conditions: (1) 25 mM Tris, (2) artificial sea water (ASW, 445 mM NaCl, 60 mM $MgCl_2$, 10 mM KCl, 10 mM $CaCl_2$, 2.4 mM $NaHCO_3$, 10 mM Hepes, pH 8.0 (Szulgit and Shadwick 2000)), (3) 25 mM Tris, 450 mM NaCl, (4) 25 mM Tris, 150 mM $CaCl_2$, and (5) 25 mM Tris, 150 mM $MgCl_2$. Mixtures of full-length and truncated rSfp1 Beta C-term proteins with rSfp1 Delta or BSA were also tested. In that case, a drop of 20 µL of each protein at 0.2 mg/mL was used. After 16 h of incubation in a humid chamber, the coverslips were rinsed for 2 h with ultrapure water under shaking, stained by Coomassie blue and observed using a Zeiss Axioscope A1 microscope. To understand the effect of $CaCl_2$ on adsorption, some of the coatings prepared as described above were air dried and immersed for 1 h in 25 mM Tris supplemented with 25 mM or 150 mM of the chelating agent ethylene glycol-bis(β-aminoethyl ether)-*N*,*N*,*N*′,*N*′-tetraacetic acid (EGTA), or in 25 mM Tris (for negative control), under shaking.

SEM–EDS

Footprints were collected as described in Hennebert et al. (2008). One sea star individual was put upside down in a tank filled with sea water, and tube feet were allowed to adhere firmly to glass coverslips previously cleaned with 5% HCl for a few minutes, and then to detach voluntarily, leaving footprints on the glass coverslips. Coatings formed by rSfp1 Beta C-term in ASW, in 25 mM Tris, 450 mM NaCl, or in 25 mM Tris, 150 mM $CaCl_2$, and by FA58C-Unannotated-FA58C in 25 mM Tris, 150 mM $CaCl_2$ were prepared on glass coverslips as described above. Footprints and coatings of recombinant proteins were rinsed for 2 h with ultrapure water under shaking and air dried. The coverslips were mounted on aluminum stubs, coated with gold/palladium in a sputter-coater and observed with a Jeol JMS-7200F field emission scanning electron microscope. X-ray microanalysis and elemental mapping were performed using an Oxford X-MaxN energy-dispersive spectrometer (EDS) equipped with an 80 mm^2 silicon drift detector. Acquisition conditions on the SEM were 5 kV, 10 mm working distance, and 10 s live time acquisition at approximately 15% dead time. The spectra were acquired with an AZtec (Oxford Instrument) EDS data processing software.

Results

Quantitative Adsorption Analysis of rSfp1 Beta C-Term and rSfp1 Delta by Surface Plasmon Resonance

Under conditions in which recombinant Sfp1 proteins form homogenous layers, i.e., 25 mM Tris, 450 mM NaCl for rSfp1 Beta C-term and 25 mM Tris, 150 mM $CaCl_2$ for rSfp1 Delta (Lefevre et al. 2020), rSfp1 Beta C-term exhibited a significantly higher adsorption than the fibrinogen and BSA controls on all investigated surface chemistries, while rSfp1 Delta adsorbed significantly more on OH, COO^-, $N(CH_3)_3^+$, and mPEG surfaces compared to both controls. BSA exhibited the lowest levels of surface adsorption on all investigated surfaces (Figs. 2, S2, S3 and Tables S2, S3 and S4). In 25 mM Tris, 450 mM NaCl, the amount of rSfp1 Beta-C term adsorbed on CH_3 (279 ng/cm^2) was similar to that adsorbed on mPEG (239 ng/cm^2) and significantly higher than on COO^- (157 ng/cm^2), OH (134 ng/cm^2), and $N(CH_3)_3^+$ (118 ng/cm^2). In this condition, fibrinogen adsorbed more on CH_3 (174 ng/cm^2) than on mPEG (79 ng/cm^2) and weakly on OH (17 ng/cm^2), COO^- (24 ng/cm^2), and $N(CH_3)_3^+$ (23 ng/cm^2). As for BSA, the quantity of adsorbed protein was higher on CH_3 (53 ng/cm^2) than on the other surfaces (between 5 and 28 ng/cm^2) (Tables S2, S3 and S5). In 25 mM Tris, 150 mM $CaCl_2$, larger amounts of rSfp1 Delta adsorbed on COO^- with 469 ng/cm^2, while the quantity of adsorbed proteins was similar on the other surfaces with 147, 139, 157, and 152 ng/cm^2 respectively for OH, CH_3, $N(CH_3)_3^+$, and mPEG. In these conditions, fibrinogen adsorbed significantly more on COO^- than on other surfaces (Tables S2, S4 and S5).

Production of Truncated rSfp1 Beta C-Term

Among the two recombinant proteins analyzed in SPR, rSfp1 Beta C-term showed the best adsorption abilities. To further characterize this protein, truncated rSfp1 Beta C-term proteins were produced (Figs. 1 and S1). As for rSfp1 Beta C-term, these 4 shorter proteins were expressed in inclusion bodies. SDS-PAGE analysis followed by Coomassie blue staining showed a high purity of the recombinant proteins (Fig. S4). The identity of the purified proteins was confirmed by mass spectrometry, which showed a sequence coverage of 85.2%, 80.5%, 73.1%, and 86% for Unannotated, FA58C, FA58C-EGF, and FA58C-Unannotated-FA58C, respectively (matched peptides are shown in bold in Fig. S1 and raw data are presented in Table S6). Purification and dialysis steps were performed either in the presence or the absence of NaCl. Indeed, although NaCl is classically used to prevent unspecific binding of the proteins to the column in metal-affinity chromatography, it was shown in our previous study that NaCl triggers the self-assembly and precipitation of rSfp1 Beta C-term (Lefevre et al. 2020). After several tests summarized in Table S7, we selected the best purification conditions as follows: in the presence of NaCl for FA58C and FA58C-EGF, and in the absence of NaCl for FA58C-Unnanotated-FA58C. Unfortunately, Unannotated precipitated completely in both purification conditions, and we could not use this protein for further experiments. The direct dialysis against Tris buffer provided the best results for the three remaining proteins (Table S7). FA58C was present in the form of soluble oligomers, FA58C-EGF was present as a mix of soluble monomers and oligomers, and FA58C-Unannotated-FA58C formed soluble oligomers (Fig. 1b). As the monomeric form was present for FA58C-EGF, the

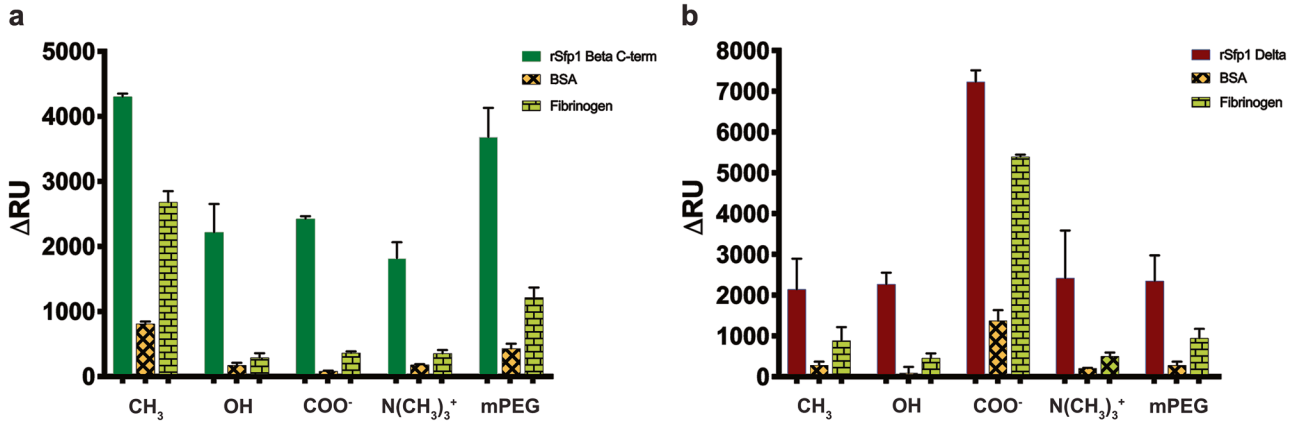

Fig. 2 SPR analysis of total protein adsorption on self-assembled monolayers (SAMs) under conditions in which rSfp1 Beta C-term (**a**) and rSfp1 Delta (**b**) form homogeneous coatings (see Lefevre et al. 2020). Data are in absolute changes in resonance units (ΔRU) after a 5-min injection of 0.5 mg/mL protein in 25 mM Tris, 450 mM NaCl, pH 8.0 (**a**), or 25 mM Tris, 150 mM $CaCl_2$, pH 8.0 (**b**) at 10 µL/min flow rate and 25 °C, followed by 1 min wash with corresponding buffer. Standard errors are from three replicate SPR experiments

behavior of this protein was observed in the presence of 450 mM NaCl, 150 mM $CaCl_2$, or 150 mM $MgCl_2$, but no difference in electrophoretic profiles was observed (Fig. S5).

Qualitative Adsorption Analysis of Truncated rSfp1 Beta C-Term Proteins

Surface coating analysis was used to qualitatively assess and compare the adsorption ability of full-length and truncated rSfp1 Beta C-term on glass under different conditions (Figs. 3 and S6; see also Lefevre et al. 2020). As for full-length rSfp1 Beta C-term, a very low adsorption was observed for the truncated proteins in the storage Tris buffer (Fig. 3a, f, k, p). rSfp1 Beta C-term adsorbed in all other tested conditions, forming a meshwork in ASW and Tris buffer supplemented with 150 mM $CaCl_2$ or $MgCl_2$ and a dense homogeneous layer in Tris buffer supplemented with 450 mM NaCl (Fig. 3b–e). FA58C adsorbed scarcely in ASW and in Tris buffer supplemented with 450 mM NaCl and did not show a notable adsorption in the presence of $CaCl_2$ or $MgCl_2$ (Fig. 3g–j). FA58C-EGF adsorbed in the form of a meshwork in ASW and Tris buffer supplemented with 150 mM $CaCl_2$ or $MgCl_2$, while almost no adsorption in the presence of NaCl was observed (Fig. 3l–o). As for FA58C-Unannotated-FA58C, it adsorbed as a meshwork in all tested conditions (Fig. 3q–t). To understand the effect of Ca^{2+} on adsorption abilities, the coatings formed by FA58C-EGF and FA58C-Unannotated-FA58C in ASW and in 25 mM Tris, 150 mM $CaCl_2$ were submitted to a treatment with increasing concentrations of the calcium-chelating agent EGTA. In all cases, this treatment led to the removal of most of the proteins adsorbed on the glass surface (Fig. S7).

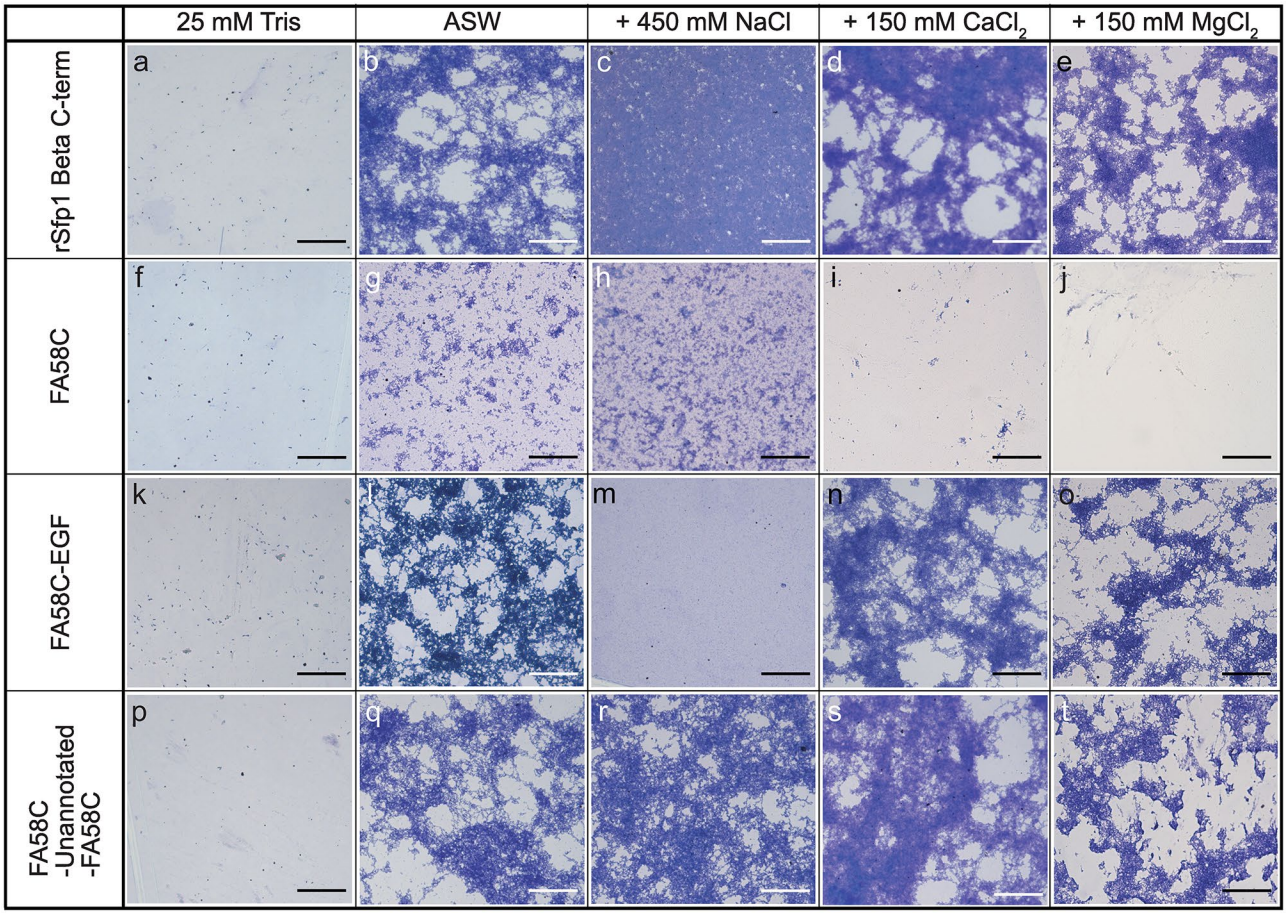

Fig. 3 Light microscopy analysis of the coatings formed by rSfp1 Beta C-term (**a**–**e**), FA58C (**f**–**j**), FA58C-EGF (**k**–**o**) and FA58C-Unannotated-FA58C (**p**–**t**) on glass. Proteins were prepared in 25 mM Tris (**a**, **f**, **k**, **p**), in artificial sea water (ASW; **b**, **g**, **l**, **q**), or in 25 mM Tris supplemented with 450 mM NaCl (**c**, **h**, **m**, **r**), 150 mM $CaCl_2$ (**d**, **i**, **n**, **s**), or 150 mM $MgCl_2$ (**e**, **j**, **o**, **t**). Scale bars 40 µm

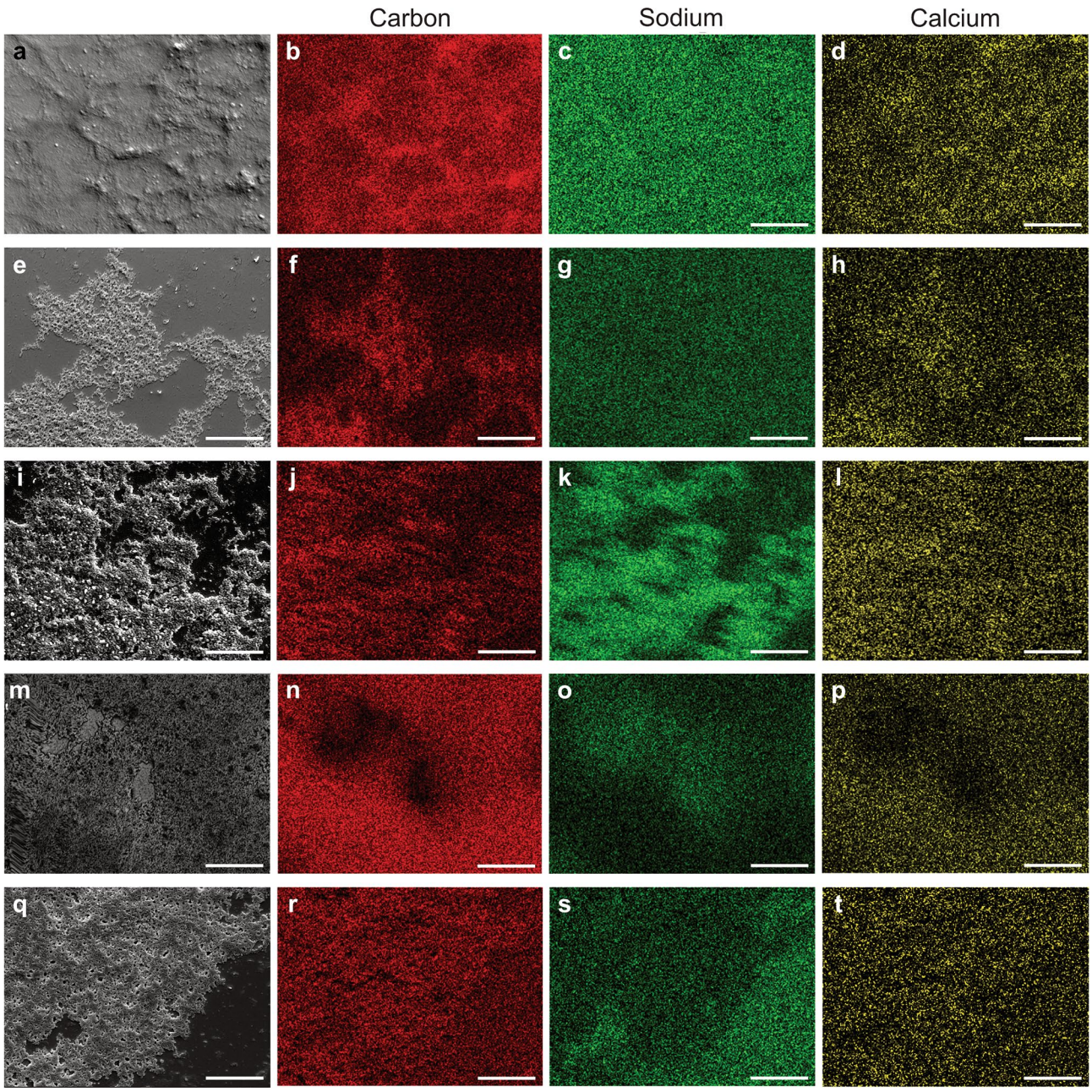

Fig. 4 Energy-dispersive spectroscopy (EDS) analyses of a sea star footprints and of recombinant protein coatings. SEM images (**a**, **e**, **i**, **m**, **q**) and corresponding EDS elemental maps showing detection of carbon (red), sodium (green), and calcium (yellow) of an air-dried footprint (**a**–**d**), and coatings formed by rSfp1 Beta C-term in ASW (**e**–**h**), rSfp1 Beta C-term in 450 mM NaCl (**i**–**l**), rSfp1 Beta C-term in 150 mM $CaCl_2$ (**m**–**p**), FA58C-Unannotated-FA58C in 150 mM $CaCl_2$ (**q**–**t**). Scale bar 5 µm

Localization of Na^+ and Ca^{2+} Ions in rSfp1 Beta C-Term and FA58C-Unannotated-FA58C Coatings and in Fresh Footprints by EDS

EDS elemental mapping was used to investigate qualitatively the localization of Na^+ and Ca^{2+} ions in air-dried sea star adhesive footprints (Fig. 4a–d), in coatings formed by rSfp1 Beta C-term in ASW (Fig. 4e–h), in 25 mM Tris supplemented with 450 mM NaCl (Fig. 4i–l), or in 25 mM Tris supplemented with 150 mM $CaCl_2$ (Fig. 4m–p), and in coatings formed by FA58C-Unannotated-FA58C in 25 mM Tris supplemented with 150 mM $CaCl_2$ (Fig. 4q–t). Carbon distribution was also investigated to visualize the location of the protein coating on the glass surface. For a more quantitative estimation of the cation content in the coatings, the weight % values of Na and Ca were normalized to the C values to account for

different protein content and distribution in the coating images (Table S8). In the native sea star adhesive footprint, the EDS analysis demonstrated the co-localization of Ca^{2+} with the fibrillar meshwork (Fig. 4b, d), while Na^{+} was found everywhere in the footprint (Fig. 4c). A similar result was observed for rSfp1 Beta C-term in ASW with Ca^{2+} co-localizing with C while Na^{+} is distributed on both the glass surface and the protein coating (Fig. 4f–h). However, the relative amount of Na^{+} and Ca^{2+} was higher in the rSfp1 Beta C-term coating than in the footprint (Table S8). For rSfp1 Beta C-term prepared in 450 mM NaCl, a high content of Na^{+} was detected, which completely co-localized with C (Fig. 4i, j, k), while no Ca^{2+} was detected, as expected (Fig. 4l and Table S8). Finally, for rSfp1 Beta C-term and FA58C-Unannotated-FA58C (i.e., rSfp1 Beta C-term without the EGF domain) in 150 mM $CaCl_2$, a high content of Ca^{2+} was detected and co-localized with C (Fig. 4m, n, p, q, r, t) while the small amounts of Na^{+} detected appear to localize on the glass surface (Fig. 4o, s and Table S7). A higher Ca/C ratio was calculated for FA58C-Unannotated-FA58C than for rSfp1 Beta C-term (Table S8).

Interaction Between rSfp1 Beta C-Term and rSfp1 Delta

To investigate the ability of Sfp1 Beta C-term and Sfp1 Delta to bind to each other, mixtures of full-length and truncated rSfp1 Beta C-term with rSfp1 Delta were analyzed by Native-PAGE and surface coating analysis on glass. In all cases, a similar electrophoretic profile was observed in Native-PAGE, where the monomeric and dimeric forms of rSfp1 Delta were observed, as well as oligomers corresponding to full-length or truncated rSfp1 Beta C-term (Fig. S8). However, a more intense staining of the interface between the stacking and the running gels was observed with FA58C. The coatings corresponding to these mixtures had the same appearance as for the full-length or truncated rSfp1 Beta C-term proteins alone (although with a more diluted aspect in the case of meshwork patterns), except for FA58C which formed a meshwork in all conditions (i.e., in ASW or 25 mM Tris buffer supplemented 450 mM NaCl or 150 mM $CaCl_2$) when mixed with rSfp1 Delta (Fig. 5). To confirm the specific interaction between FA58C and rSfp1 Delta, the same experiment was performed by replacing rSfp1 Delta by BSA. In that case, no adsorption was observed on the glass surface (Fig. S9a–c).

Discussion

Protein adsorption is studied in various fields such as biotechnology, medicine, or food industry, with the aim to prevent it or, on the contrary, to increase it for specific purposes (see Nakanishi et al. 2001; Ngo and Grulan 2017 for reviews). Among these purposes, the ability of proteins to adsorb to fluid-bathed surfaces is a particular concern, for instance, to facilitate the attachment of cells that will allow the proper integration of implantable medical devices (Wilson et al. 2005). Adhesive secretions from marine invertebrates are an important source of inspiration for such applications (Claverie et al. 2020). Recently, we showed that recombinant multimodular proteins inspired from the sea star adhesive protein Sfp1, rSfp1 Beta C-term, and rSfp1 Delta self-assemble in the presence of NaCl, and adsorb on glass and polystyrene surfaces upon addition of different types of salts. Depending on the buffer condition (i.e., the type of salt used and its concentration), the recombinant proteins form either homogeneous coatings or irregular meshworks (Lefevre et al. 2020). We showed that the homogeneous coatings are biocompatible and enable cell proliferation (Lefevre et al. 2020).

In this study, we used surface plasmon resonance (SPR) to characterize quantitatively the adsorption abilities of the two Sfp1 recombinant proteins on hydrophobic (CH_3), hydrophilic (OH), hydrophilic protein-resistant (mPEG), and negatively (COO^{-}) and positively ($N(CH_3)_3^{+}$) charged surfaces under conditions showing the formation of the most homogenous protein layers (i.e., 25 mM Tris, 450 mM NaCl, pH 8 for rSfp1 Beta C-term, and 25 mM Tris, 150 mM $CaCl_2$, pH 8 for rSfp1 Delta). The amounts of adsorbed proteins were compared to BSA and to fibrinogen, two proteins often used as model proteins for molecular adhesion research because their adsorption ability is known on a wide range of surfaces, including non-fouling surfaces like poly(ethylene glycol) (PEG) (Lowe et al. 2015; Kubiak-Ossowska et al. 2017; Tilbury et al. 2019). Under the tested conditions, rSfp Beta C-term showed a significantly higher adsorption on all surfaces, and rSfp1 Delta adsorbed significantly more on OH, COO^{-}, $N(CH_3)_3^{+}$, and mPEG surfaces, compared to BSA and fibrinogen. At the pH of the buffers used for the experiments, all proteins possessed a net-negative charge (pI = 6.2, 4.3, 5.8, and 5.7 for rSfp1 Beta C-term, rSfp1 Delta, fibrinogen, and BSA, respectively). The fact that high amounts of both recombinant proteins adsorbed onto different types of surfaces (either neutral, or positively or negatively charged) demonstrates that protein charge and electrostatic interactions alone do not explain the adsorption ability of these two proteins, and that other types of interactions are involved. The amounts of recombinant proteins adsorbed (between 118 and 460 ng/cm^2 according to the protein and the surface) were largely higher than those observed for the barnacle rPpolcp19k (between 1 and 45 ng/cm^2; Tilbury et al. 2019) and in the same range as those measured for the barnacle cyprid settlement-inducing protein complex (SIPC; Petrone et al. 2015) with SPR on the same types of surfaces, although the comparison in the latter case is complicated by the much lower SIPC protein concentrations ($\leq$0.1 mg/mL)

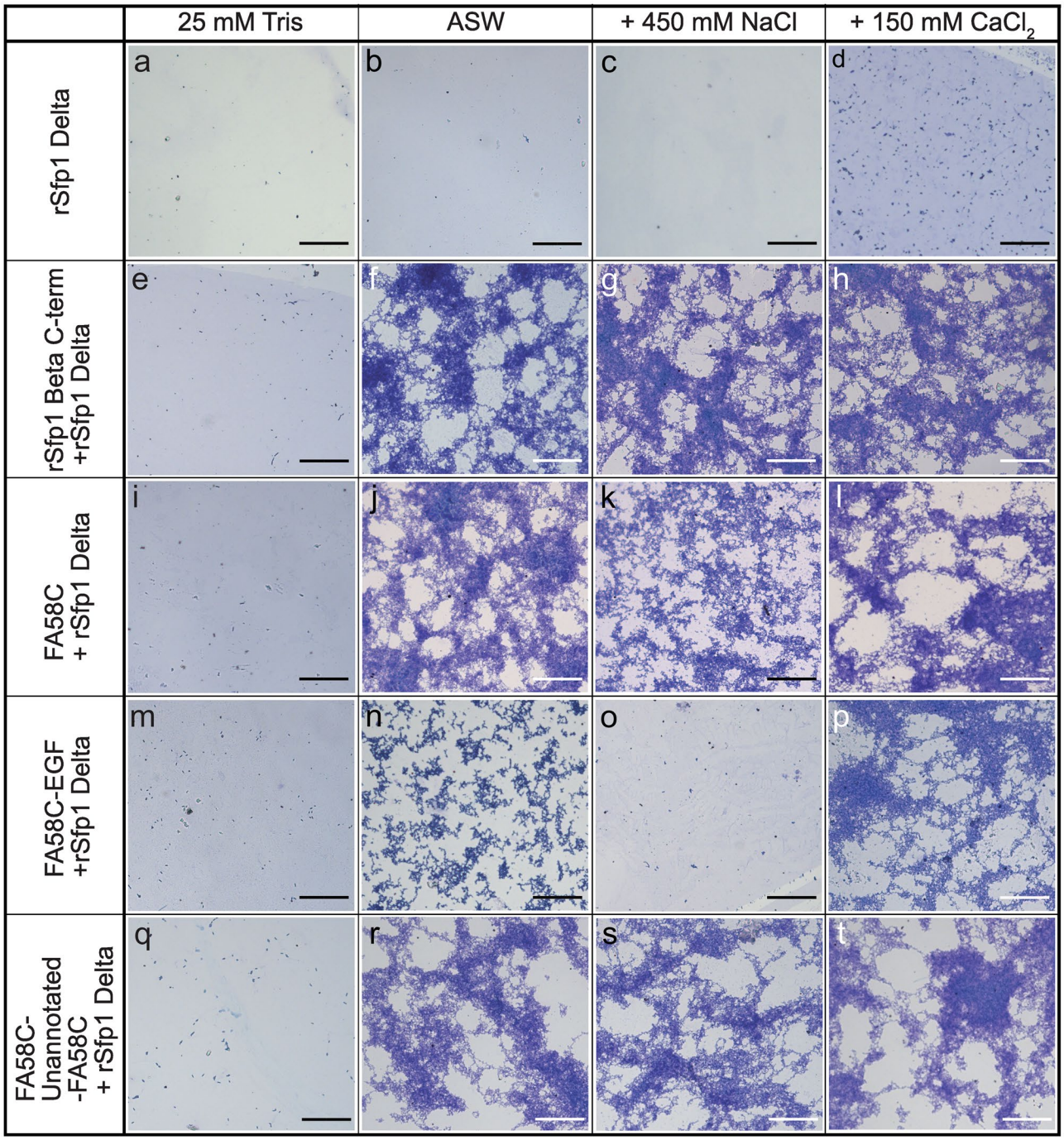

Fig. 5 Light microscopy analysis of the coatings formed by rSfp1 Delta alone (**a**–**d**) or mixed with rSfp1 Beta C-term (**e**–**h**), FA58C (**i**–**l**), FA58C-EGF (**m**–**p**), or FA58C-Unannotated-FA58C (**q**–**t**) on glass. Proteins were prepared in 25 mM Tris (**a**, **e**, **i**, **m**, **q**), in artificial sea water (ASW; **b**, **f**, **j**, **n**, **r**), in 25 mM Tris supplemented with 450 mM NaCl (**c**, **g**, **k**, **o**, **s**), or in 25 mM Tris supplemented with 150 mM $CaCl_2$ (**d**, **h**, **l**, **p**, **t**). Scale bars 40 µm

used by Petrone et al. (2015). The observed adsorption of the recombinant proteins is also similar to, or higher than that observed for mussel foot protein Mefp-1 on methyl-terminated surfaces by ellipsometry and SPR, viz. 130–165 ng/cm^2 (Höök et al. 2001). Interestingly, the adsorption ability of recombinant Sfp1 proteins on a high diversity of surfaces could reflect, to some extent, the versatility of the native sea star adhesive, thereby explaining the ability of sea stars to attach to different types of surfaces encountered during their displacements (Santos et al. 2009).

High amounts (134–239 ng/cm^2) of both rSfp1 Beta C-term and rSfp1 Delta adsorbed on OH and mPEG, where the latter is generally considered very protein resistant (Prime and Whitesides 1993). This might indicate remarkable adsorption abilities of the rSfp1 recombinant proteins, although the adsorption also of the control proteins to the mPEG surfaces was overall relatively high. For example, the amounts of fibrinogen adsorbed on mPEG surfaces under the tested conditions were higher than on oligo(ethylene glycol) (OEG) surfaces in Tris buffer alone or in Tris buffer supplemented with NaCl (Petrone et al. 2015; Tilbury et al. 2019). The protein resistance of PEG (and mPEG) is usually evaluated under physiological conditions, and it is possible that the considerably different buffer conditions (450 mM NaCl, or 150 mM $CaCl_2$) adversely affect the structure or the hydration properties of the mPEG polyether chains, with ensuing deterioration of the protein adsorption resistance (Harder et al. 1998; Wang et al. 2000). Similarly, when salinity and pH differ from those at physiological conditions, the properties of the proteins are affected, possibly leading to conformational changes or even denaturation, and changes in bulk pH and Debye screening length will also affect direct protein-surface interactions. For the charged SAMs, hydration and charge regulation determining net surface charge will be affected. These effects will undoubtedly affect the results of the adsorption study and might contribute to the high adsorption onto the mPEG. However, the importance of each of these factors is not easily disentangled with the currently available data.

The interpretation of the adsorption data inferred from the SPR sensorgrams (Figs. S2 and S3) is complicated by the presence of mass-transport limited adsorption (Figs. S2c and S3a), and biphasic response curves (Figs. S2d and S3c, e), some with possible mass-transport limitations in the second phase. Mass-transport limitations lead to underestimation of the adsorbed amount, for otherwise comparable experimental conditions, and since this is most prominent for some of the recombinant protein sensorgrams, it is probable that some of the reported adsorbed amounts are underestimated, for the given conditions. The available amounts of recombinant proteins set limits to the experimental conditions (protein concentration, flow rate, saturation) and did not allow a full investigation of these effects, or the determination of rate constants. For example, comparing the responses of rSfp Beta C-term and rSfp1 Delta on the two charged SAMs, we note the opposite behavior of the two proteins on the carboxyl- and trimethyl amine SAMs. Where rSfp Beta C-term has a distinct bi-phasic behavior on the trimethyl amine SAM but not on the carboxylated surface, rSfp1 Delta shows the opposite behavior, indicating qualitatively different, and possibly coverage-dependent, orientational and/or conformational changes. In the case of rSfp1 Delta, cross-bridging of the negatively charged protein with the negatively charged carboxylated SAM through Ca^{2+} cations is undoubtedly involved in the fast initial adsorption.

Next, we decided to investigate further the adsorption of rSfp1 Beta C-term by producing truncated proteins in order to understand the respective roles of its FA58C (discoidin), calcium-binding EGF, and Unannotated domains. First, it should be noted that, although all recombinant proteins oligomerized, the differences observed in our adsorption tests (presence or absence of adsorption, adsorption in the form of a homogeneous layer or of a meshwork) tend to demonstrate that adsorption is due to specific interactions and is not only a result of aggregation. The FA58C (discoidin) domain exhibited only a weak adsorption ability on glass, showing that it is not important for this function. However, its role in Sfp1 adhesion should not be neglected, as it is repeated five times in Sfp1 Beta and is also the only functional domain, repeated six times, in Nectin, an adhesive protein from sea urchins (Toubarro et al. 2016; Pjeta et al. 2020). In our previous study, we proposed that this discoidin domain could interact with the von Willebrand factor (comprising VWD, C8, and TIL domains) of the Delta (and also the Gamma) subunit of Sfp1 to allow cross-linking between several Sfp1 (Lefevre et al. 2020). The analysis of the mixture of FA58C and rSfp1 Delta in Native-PAGE did not conclusively corroborate this hypothesis. Indeed, although more abundant oligomers were present at the entry of the running gel, the monomer and dimer forms of rSfp1 Delta were still visible on the gel. However, as the Native-PAGE analysis was performed in Tris buffer, this observation does not exclude the possibility of a binding between the two subunits mediated by some ions. Indeed, in ASW and in the presence of NaCl and $CaCl_2$, the mix of FA58C and rSfp1 Delta adsorbed on the glass surface.

Regarding FA58C-EGF, its adsorption was triggered by the addition of $CaCl_2$ or $MgCl_2$ to the Tris buffer, or by ASW (which contains, among others, 445 mM NaCl, 60 mM $MgCl_2$, and 10 mM $CaCl_2$), but not by the addition of NaCl. However, Native-PAGE analysis showed that the addition of $CaCl_2$ and $MgCl_2$ did not cause the complete oligomerization of this protein. Altogether, it seems that the calcium-binding EGF-like domain is involved in the binding of Sfp1 Beta to the surface, this binding being mediated by Ca^{2+} or Mg^{2+} ions. To verify this hypothesis, we incubated FA58C-EGF coatings with EGTA, a compound which chelates Ca^{2+} ions with a high affinity, but also Mg^{2+} ions to some extent (Sorour et al. 2016). Increasing amounts of this chelating agent almost completely removed the FA58C-EGF coating. Although the role of Ca^{2+} is obvious for the calcium-binding EGF domain, that of Mg^{2+} is not.

Finally, as FA58C did not show adsorption ability, it is tempting to conclude that the role of the Unannotated domain could be inferred from the analysis of the FA58C-Unannotated-FA58C fragment, which also corresponds to

rSfp1 Beta C-term without the EGF domain. However, one could not exclude the possibility that the association of several FA58C domains could improve the adsorption abilities, as observed in Nectin recombinant proteins (Da Costa et al. 2016). FA58C-Unannotated-FA58C adsorbed in ASW and in the presence of NaCl, $CaCl_2$, and $MgCl_2$. As for FA58C-EGF, the role of divalent cations in the adsorption ability of the FA58C-Unannotated-FA58C fragment was confirmed by the removal of the coating after addition of EGTA. Together with the co-localization of Ca^{2+} and proteins in FA58C-Unannotated-FA58C coating in EDS maps, these results indicate that the EGF domain is not the only domain from Sfp1 Beta interacting with divalent cations. The unannotated sequence comprises more valine (10.2%), serine (10.7%), arginine (7.5%), and glycine (7.5%) than an average eucaryote protein (Bogatyreva et al. 2006; Gaur 2014) (Table S9). Although our results do not allow explaining the mechanisms triggering adsorption of this unannotated sequence, comparison with other marine adhesive proteins allow proposing some hypotheses. In the barnacle cement protein cp19k, it has been proposed that the abundant Gly residues are responsible for the disordered structure of the protein, thereby favoring its unspecific adsorption to various surfaces (Wang et al. 2018). Interestingly, circular dichroism analysis of rSfp1 Beta C-term revealed a prevalence of β-sheet and random coil structures. It has been suggested that the β-sheet structures correspond to the secondary structures of the functional domains found in the proteins whereas the random coils could derive from the unannotated portions of the proteins (Lefevre et al. 2020). In cp19k, serine and valine residues have been shown to bind to hydrophilic surfaces by replacing surface-bound water through their hydroxyl or/and methyl groups (Petrone 2013; Wang et al. 2018). Finally, the arginine residues, which are charged at pH 8, could be involved in electrostatic interactions with the surface. The fact that post-translational modifications are not performed in bacterial expression system (Sharifi-Sirchi and Jalali-Javaran 2016) exclude the possibility that such modifications would be involved in the adsorption of this peculiar sequence with no similarity in databases. Contrary to FA58C alone, FA58C-EGF and FA58C-Unannotated-FA58C did not seem to bind to rSfp1 Delta in the absence of salts in Native-PAGE. Moreover, the aspect of the coatings was not modified much after the addition of Sfp1 Delta, except for the fact that the meshwork formed appeared less dense. This could be explained by the fact that twice less of proteins were used in the case of mixtures. Therefore, the EGF and the Unannotated domains do not seem to be involved in interactions between the Beta and the Delta subunits of Sfp1.

Noteworthy, we were not able to perform shear tests to evaluate the adhesivity of the rSfp1 coatings. Indeed, although the proteins adsorbed to glass surfaces, they were unable to bind two glass surfaces together, even after prolonged contact time. This is consistent with the very low adhesion force (about 100 pN) measured with PeakForce Quantitative Nanomechanical Property Mapping Atomic Force Microscopy (Lefevre et al. 2021). As observed for the mussel proteins mfp-1 and mfp-3 (Lin et al. 2007), these results are consistent with the function of Sfp1 in the native glue, where it acts as a cohesive protein and probably interacts with at least another adhesive protein which binds to the surface.

Together with the results obtained in our previous study (Lefevre et al. 2020), the present results demonstrate the ability of Sfp1 to adsorb to a large variety of surfaces, thereby reinforcing its biotechnological potential as a coating material. For instance, as the protein films obtained were shown to have no cytotoxic effects and even increased cell proliferation (Lefevre et al. 2020), they could be used to functionalize medical implants to favor wound repair and tissue integration (Wilson et al. 2005). Moreover, we showed that even small fragments of Sfp1 are promising for such applications, in particular the unannotated sequence. This could facilitate the implementation of Sfp1-inspired coatings.

Supplementary Information The online version contains supplementary material available at https://doi.org/10.1007/s10126-021-10059-y.

Acknowledgements The authors want to thank Cyril-Terence Mascolo and Dr. Corentin Decroo for their advice on the mass spectrometry experiments.

Author Contribution Mathilde Lefevre: investigation, writing—original draft. Patrick Flammang: conceptualization, investigation, writing — review and editing. Thibault Masai: investigation. Ruddy Wattiez: investigation. Thomas Ederth: investigation, writing — review and editing. Philippe Leclère: writing — review and editing. Elise Hennebert: conceptualization, supervision, writing — original draft.

Funding This research was supported by the ARC project "PROTEST" (Production and testing of recombinant sea star adhesive proteins; "Fédération Wallonie-Bruxelles – Actions de Recherche Concertées", ARC-17/21 UMONS 3), by the European Cooperation in Science and Technology (COST) Action CA15216 (STSM n°36,087, 41,592 and 45,324), by the Fund for Scientific Research of Belgium (F.R.S.-FNRS) "Projet de Recherche" T.0088.20, and by the Fund for Medical Research in Hainaut (F.R.M.H.). The bioprofiling platform used for the de novo sequencing analysis was supported by the European Regional Development Fund and the Walloon Region. P.F. and P.L. are Research Directors of the F.R.S.- FNRS.

Declarations

Ethics Approval Not applicable.

Consent to Participate Not applicable.

Consent for Publication Not applicable.

Conflict of Interest The authors declare no competing interests.

References

Bogatyreva NS, Finkelstein AV, Galzitskaya OV (2006) Trend of amino acid composition of proteins of different taxa. J Bioinform Comput Biol 04:597–608

Claverie M, McReynolds C, Petitpas A, Thomas M, Fernandes SCM (2020) Marine-derived polymeric materials and biomimetics: an overview. Polymers (Basel, Switz.) 12:1002

Da Costa G, Toubarro D, Marquês J, Viana A, Cordeiro C, Cabral H, Santos R (2016) Expression of recombinant sea urchin-inspired adhesive proteins: discovery, production and applications. Frontiers Marine Science Conference Abstract: IMMR | International Meeting on Marine Research 2016

Flammang P, Michel A, Cauwenberge AV, Alexandre H, Jangoux M (1998) A study of the temporary adhesion of the podia in the sea star asterias rubens (Echinodermata, asteroidea) through their footprints. J Exp Biol 201:2383–2395

Gaur RK (2014) Amino acid frequency distribution among eukaryotic proteins. The IIOAB Journal 5:6–11

Harder P, Grunze M, Dahint R, Whitesides GM, Laibinis PE (1998) Molecular conformation in oligo(ethylene glycol)-terminated self-assembled monolayers on gold and silver surfaces determines their ability to resist protein adsorption. J Phys Chem B 102:426–436

Hennebert E, Leroy B, Wattiez R, Ladurner P (2015) An integrated transcriptomic and proteomic analysis of sea star epidermal secretions identifies proteins involved in defense and adhesion. J Proteomics 128:83–91

Hennebert E, Viville P, Lazzaroni R, Flammang P (2008) Micro- and nanostructure of the adhesive material secreted by the tube feet of the sea star Asterias rubens. J Struct Biol 164:108–118

Hennebert E, Wattiez R, Demeuldre M, Ladurner P, Hwang DS, Waite JH, Flammang P (2014) Sea star tenacity mediated by a protein that fragments, then aggregates. Proc Natl Acad Sci USA 111:6317–6322

Horbett TA (2018) Fibrinogen adsorption to biomaterials. J Journal of Biomedical Materials Research Part A 106:2777–2788

Höök F, Kasemo B, Nylander T, Fant C, Sott K, Elwing H (2001) Variations in coupled water, viscoelastic properties, and film thickness of a Mefp-1 protein film during adsorption and cross-linking: a quartz crystal microbalance with dissipation monitoring, ellipsometry, and surface plasmon resonance study. Anal Chem 73:5796–5804

Kubiak-Ossowska K, Tokarczyk K, Jachimska B, Mulheran PA (2017) Bovine serum albumin adsorption at a silica surface explored by simulation and experiment. J Phys Chem B 121:3975–3986

Lefevre M, Flammang P, Aranko AS, Linder MB, Scheibel T, Humenik M, Leclercq M, Surin M, Tafforeau L, Wattiez R, Leclère P, Hennebert E (2020) Sea star-inspired recombinant adhesive proteins self-assemble and adsorb on surfaces in aqueous environments to form cytocompatible coatings. Acta Biomater 112:62–74

Lefevre M, Tran TQ, De Muijlder T, Pittenger B, Flammang P, Hennebert E, Leclère P (2021) On the nanomechanical and viscoelastic properties of coatings made of recombinant sea star adhesive proteins. Frontiers in Mechanical Engineering 7:667491.

Lengerer B, Algrain M, Lefevre M, Delroisse J, Hennebert E, Flammang P (2019) Interspecies comparison of sea star adhesive proteins. Philosophical Transactions of the Royal Society b: Biological Sciences 374:20190195

Lin Q, Gourdon D, Sun C, Holten-Andersen N, Anderson TH, Waite JH, Israelachvili JN (2007) Adhesion mechanisms of the mussel foot proteins Mfp-1 and Mfp-3. Proc Natl Acad Sci USA 104:3782–3786

Lowe S, O'Brien-Simpson NM, Connal LA (2015) Antibiofouling polymer interfaces: poly(ethylene glycol) and other promising candidates. Polym Chem 6:198–212

Nakanishi K, Sakiyama T, Imamura K (2001) On the adsorption of proteins on solid surfaces, a common but very complicated phenomenon. J Biosci Bioeng 91:233–244

Ngo BKD, Grunlan MA (2017) Protein resistant polymeric biomaterials. ACS Macro Lett 6:992–1000

Petrone L (2013) Molecular surface chemistry in marine bioadhesion. Adv Coll Interface Sci 195–196:1–18

Petrone L, Aldred N, Emami K, Enander K, Ederth T, Clare AS (2015) Chemistry-specific surface adsorption of the barnacle settlement-inducing protein complex. Interface Focus 5:20140047

Pjeta R, Lindner H, Kremser L, Salvenmoser W, Sobral D, Ladurner P, Santos R (2020) Integrative transcriptome and proteome analysis of the tube foot and adhesive secretions of the sea urchin Paracentrotus lividus. Int J Mol Sci 21:946

Prime KL, Whitesides GM (1993) Adsorption of proteins onto surfaces containing end-attached oligo(ethylene oxide): a model system using self-assembled monolayers. J Am Chem Soc 115:10714–10721

Santos R, Hennebert E, Coelho AV, Flammang P (2009) The echinoderm tube foot and its role in temporary underwater adhesion. In Functional Surfaces in Biology, Dordrecht

Seear PJ, Rosato E, Goodall-Copestake WP, Barber I (2015) The molecular evolution of spiggin nesting glue in sticklebacks. Mol Ecol 24:4474–4488

Sharifi-Sirch GR, Jalali-Javaran M (2016) Selecting appropriate hosts for recombinant proteins production: review article. Hormozgan Medical Journal 20:e87690

Sorour MH, Hani HA, Shaalan HF, El-Sayed MMH (2016) Experimental screening of some chelating agents for calcium and magnesium removal from saline solutions. Desalin Water Treat 57:22799–22808

Szulgit GK, Shadwick RE (2000) Dynamic mechanical characterization of a mutable collagenous tissue: response of sea cucumber dermis to cell lysis and dermal extracts. J Exp Biol 203:1539–1550

Tilbury MA, McCarthy S, Domagalska M, Ederth T, Power AM, Wall JG (2019) The expression and characterization of recombinant Cp19k barnacle cement protein from Pollicipes pollicipes. Philosophical Transactions of the Royal Society b: Biological Sciences 374:20190205

Toubarro D, Gouveia A, Ribeiro RM, Simões N, da Costa G, Cordeiro C, Santos R (2016) Cloning, characterization, and expression levels of the nectin gene from the tube feet of the sea urchin Paracentrotus lividus. Mar Biotechnol 18:372–383

Wang RLC, Jürgen Kreuzer H, Grunze M (2000) The interaction of oligo(ethylene oxide) with water: a quantum mechanical study. Phys Chem Chem Phys 2:3613–3622

Wang X, Wang C, Xu B, Wei J, Xiao Y, Huang F (2018) Adsorption of intrinsically disordered barnacle adhesive proteins on silica surface. Appl Surf Sci 427:942–949

Wilson CJ, Clegg RE, Leavesley DI, Pearcy MJ (2005) Mediation of biomaterial–cell interactions by adsorbed proteins: a review. Tissue Eng 11:1–18

Wunderer J, Lengerer B, Pjeta R, Bertemes P, Kremser L, Lindner H, Ederth T, Hess MW, Stock D, Salvenmoser W, Ladurner PA (2019) Mechanism for temporary bioadhesion. Proc Natl Acad Sci 116:4297–4306